SAND2019-3557PE

Impact of the Microscale on Remote Sensing Signatures

Tom Reichardt, Sam Eaton, and Tom Kulp

Sandia National Laboratories

P. O. Box 969, MS 9033, Livermore, CA 94551

Presented to the Bionuclear Working Group

Sandia National Laboratories is a multimission laboratory managed and operated by National Technology and Engineering Solutions of Sandia, LLC., a wholly owned subsidiary of Honeywell International, Inc., for the U.S. Department of Energy's National Nuclear Security Administration under contract DE-NA0003525.

May 1st, 2018

Viewgraph background: The traverse cross section of a European beech leaf from Gerber et al., Rem. Sens. Environ. 115, 404-414 (2011

Silica Powders: A Visible Example of the Microscale Impact

Transitioning from the finer to the coarser powders:

- Less scattering per unit volume
- Appear less bright

Silica Powders: An Infrared Example of the Morphological Dependence

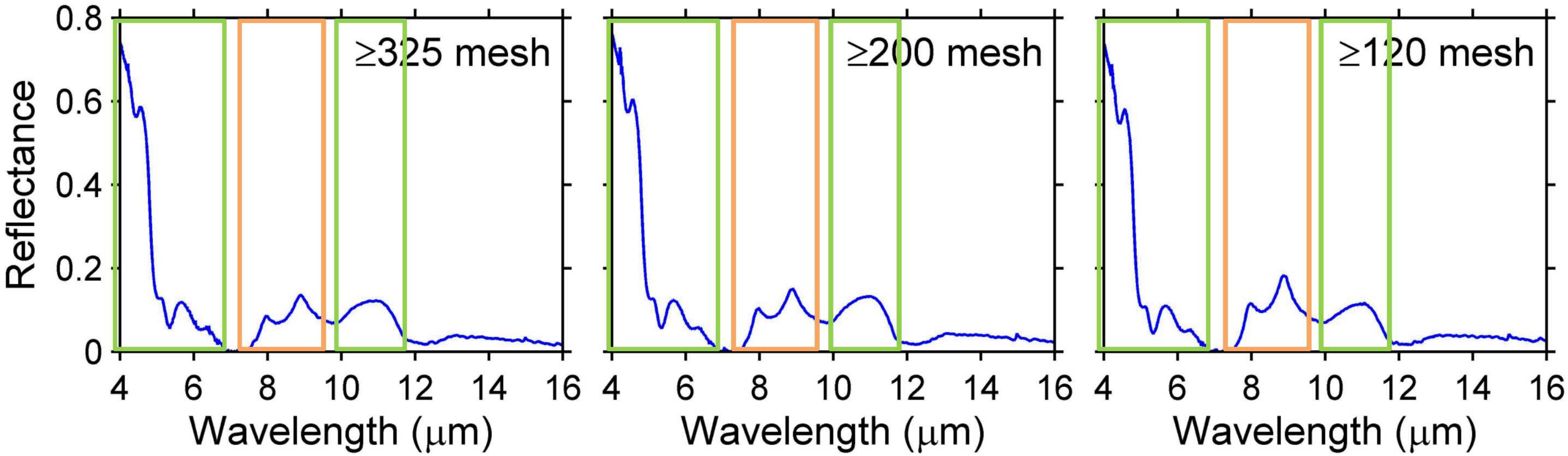

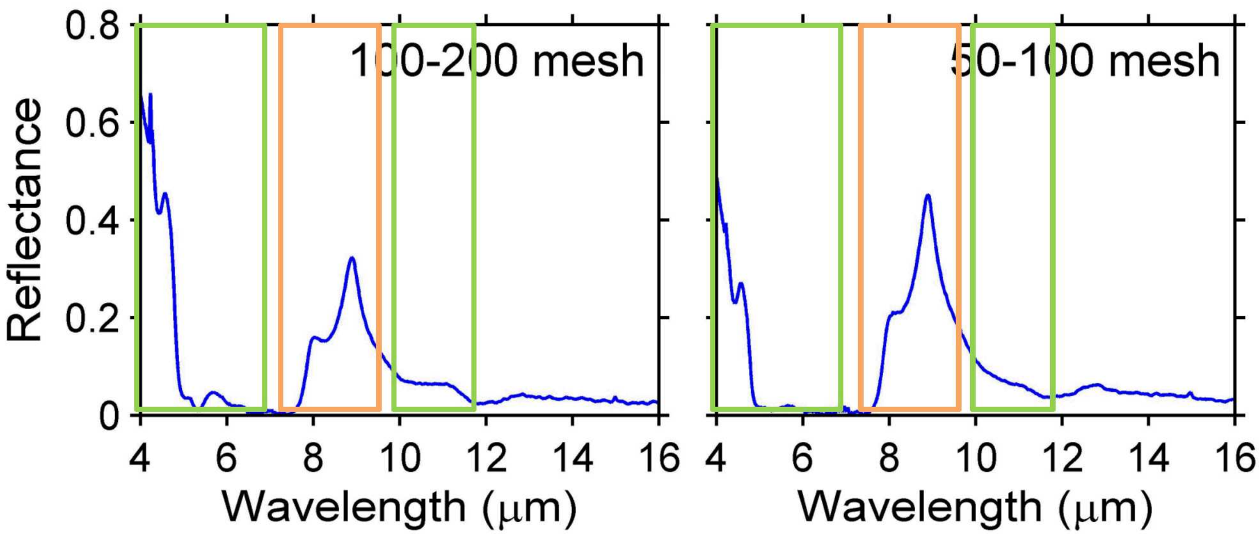

Mesh	Size (μm)
325	44
200	74
120	125
100	149
50	297

Silica Powders: An Infrared Example of the Morphological Dependence

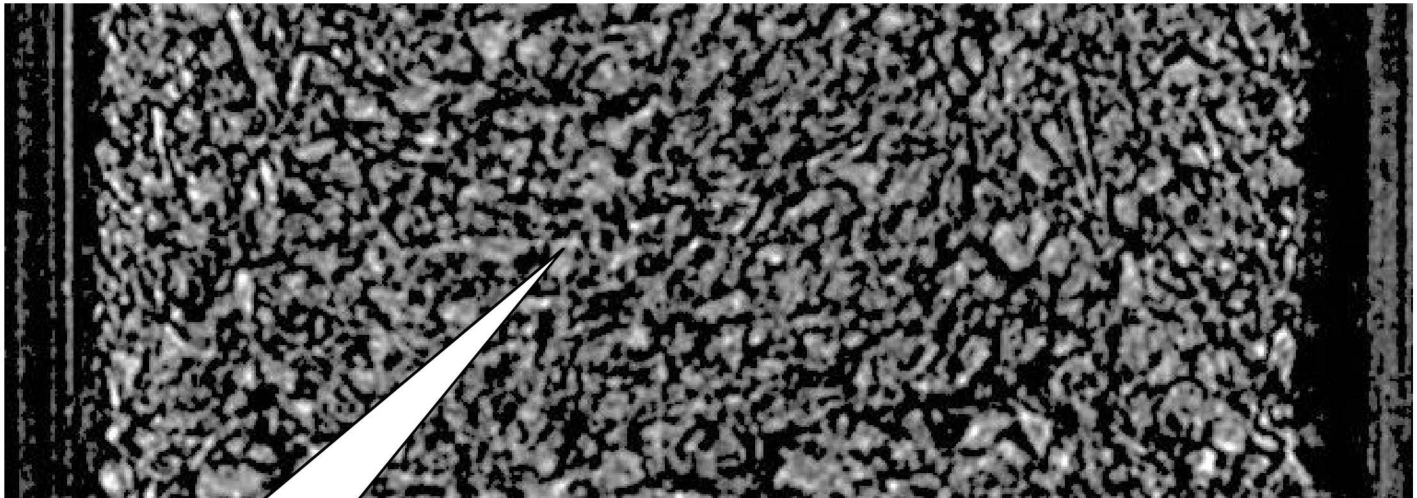

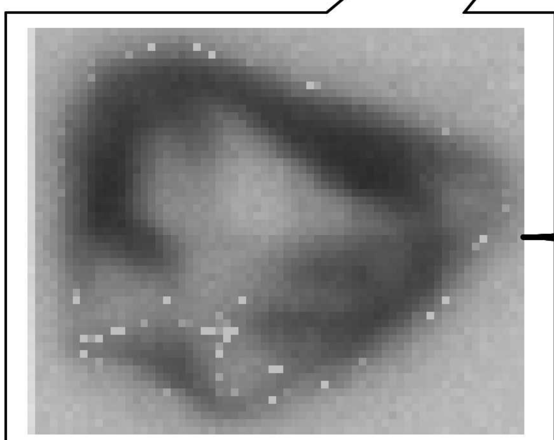

$$\nabla \cdot \mathbf{D}(\mathbf{r}) = \rho(\mathbf{r})$$
$$\nabla \times \mathbf{E}(\mathbf{r}) = i\omega\mu\mathbf{H}(\mathbf{r})$$
$$\nabla \cdot [\mu\mathbf{H}(\mathbf{r})] = 0$$
$$\nabla \times \mathbf{H}(\mathbf{r}) = \mathbf{J}(\mathbf{r}) - i\omega\mathbf{D}(\mathbf{r}) = -i\omega\varepsilon\mathbf{E}(\mathbf{r})$$

$$n + ik = c(\varepsilon\mu)^{1/2}$$

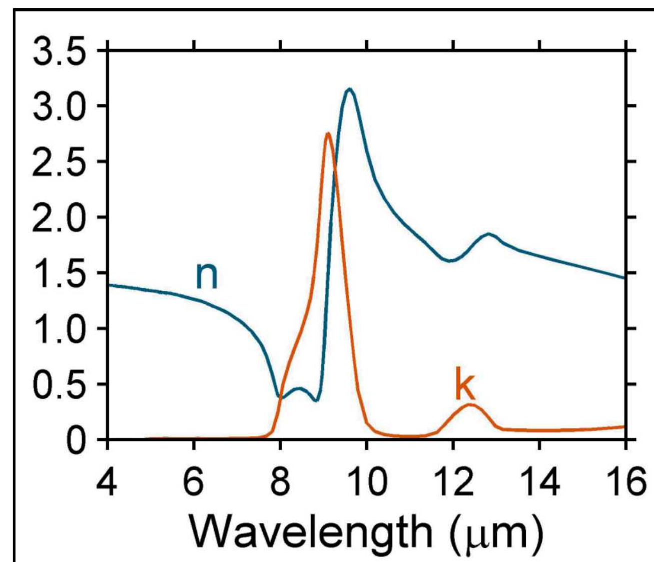

Introduce phenomenological "surface scattering" vs. "volume scattering"

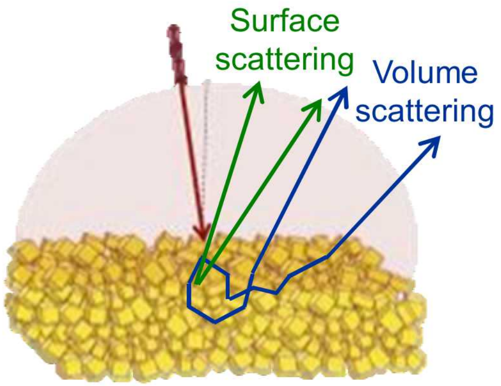

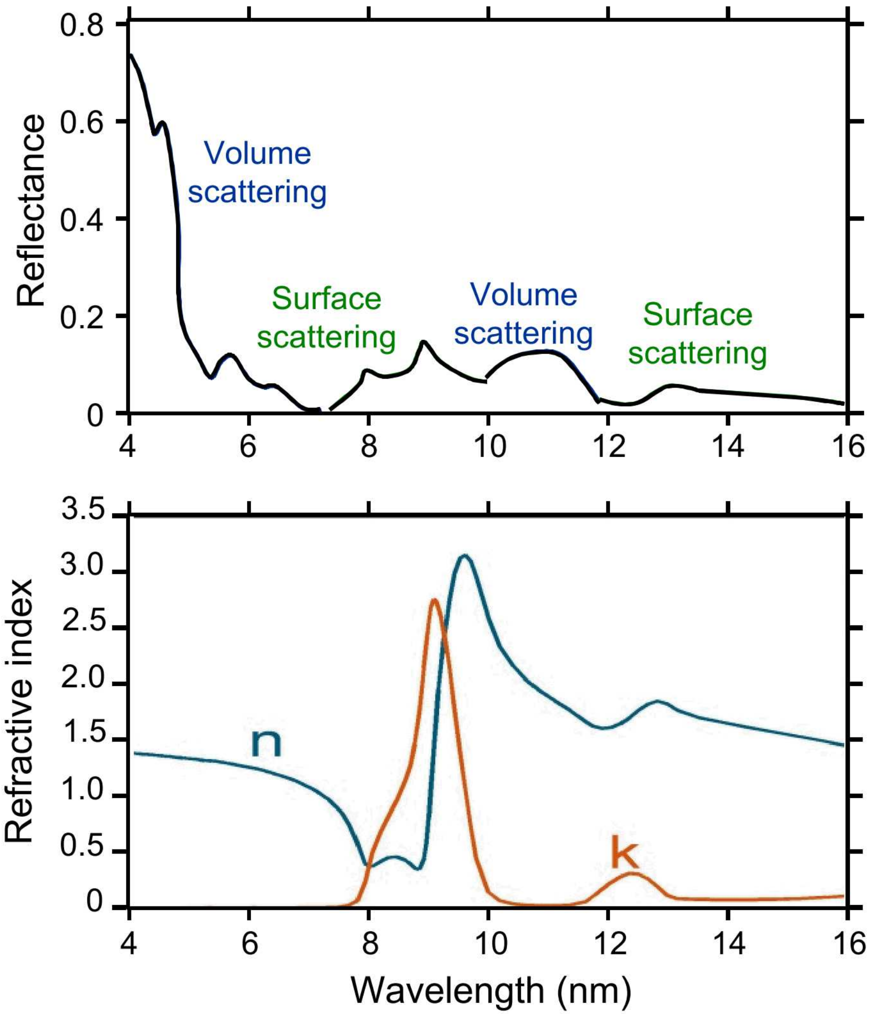

Surface scattering from particles: High k

Volume scattering from particles: Low k

Community Models: Current State-of-the-Art

G. Ito, J. A. Arnold, and T. D. Glotch, “T-matrix and radiative transfer hybrid models for densely packed particulates at mid-infrared wavelengths,” J. Geophy. Res. Planets **122**, 822-838 (2017).

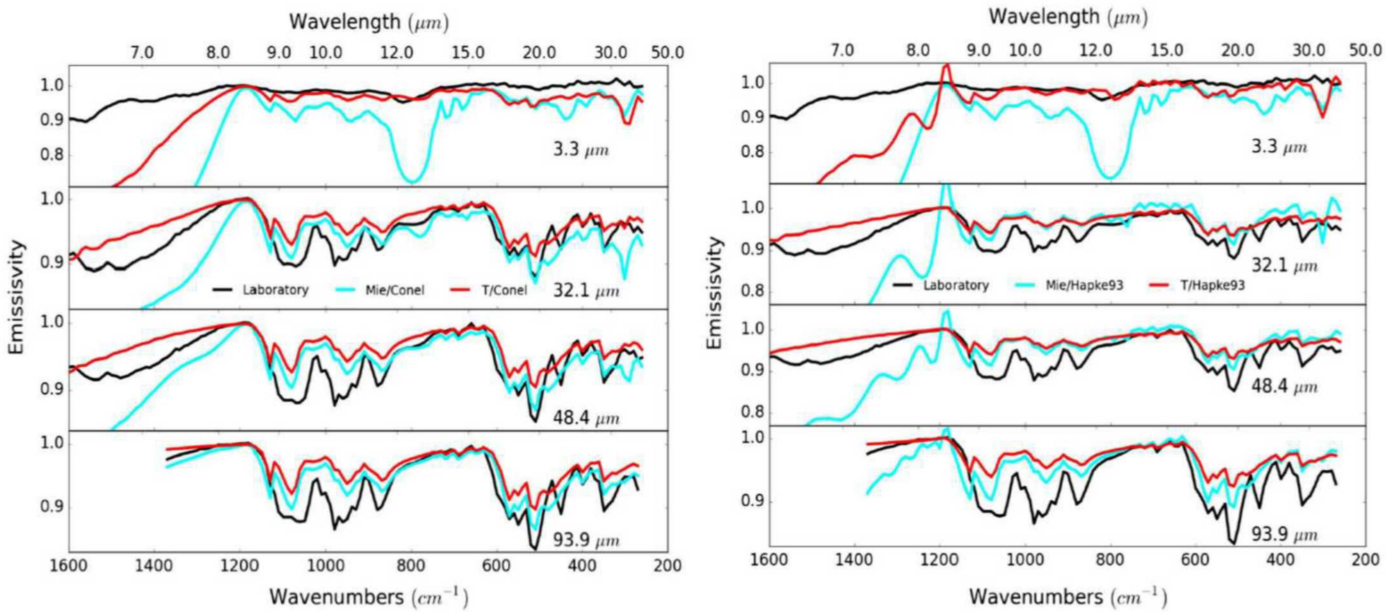

F. Rivera-Hernandez, J. L. Bandfield, S. W. Ruff, and M. J. Wolff, “Characterizing the thermal infrared spectral effects of optically thin surface dust: Implications for remote-sensing and in situ measurements of the Martian surface,” Icarus **262**, 173-186 (2015).

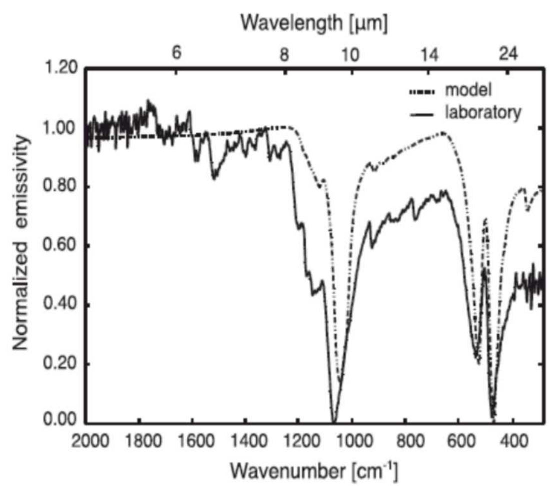

- Performance of these models deemed insufficient for high-confidence material detect/ID
- Served as key motivation for NA-22’s HARD Solids Venture

Discussion Topics

- **Forward/inverse radiative transfer (RT) model for an optically thick deposit**
  - Optimized, the model should demonstrate agreement with reflectance spectra…
  - …while the extracted parameters should agree with independent measurements
- **Initial results from a forward/inverse RT model for optically thin deposits**
- **Relevance to BNWG**

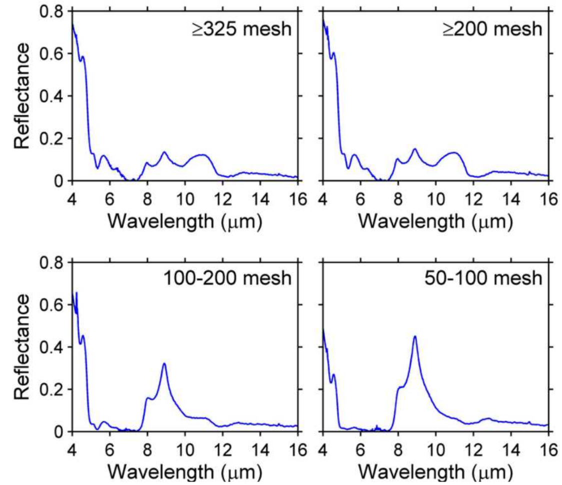

Mesh	Size (μm)
325	44
200	74
120	125
100	149
50	297

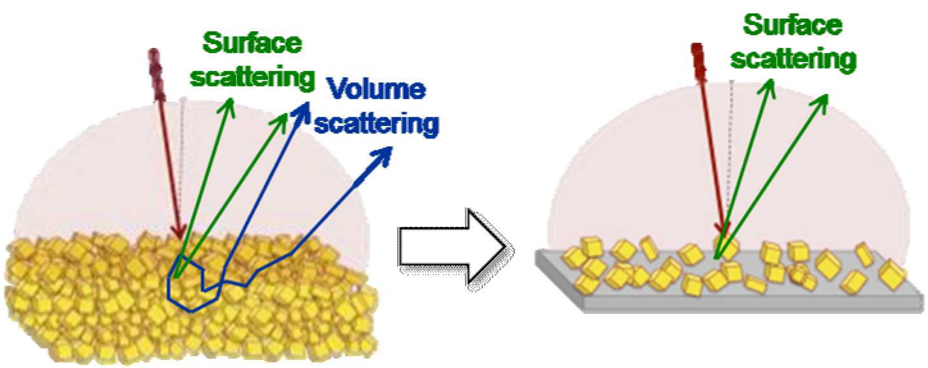

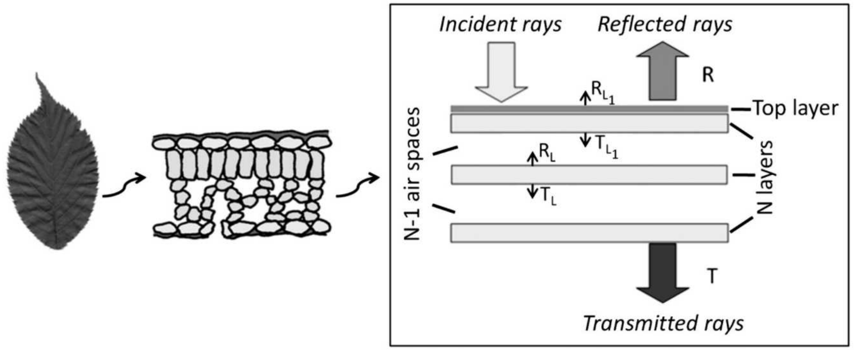

F. Gerber et al., "Modeling directional-hemispherical reflectance and transmittance of fresh and dry leaves from 0.4 um to 5.7 um with the PROSPECT-VISIR model," Rem. Sens. Environ. **115**, 404-414, 2011.

Computational Approach: The Ambartsumian Invariant Embedding Method

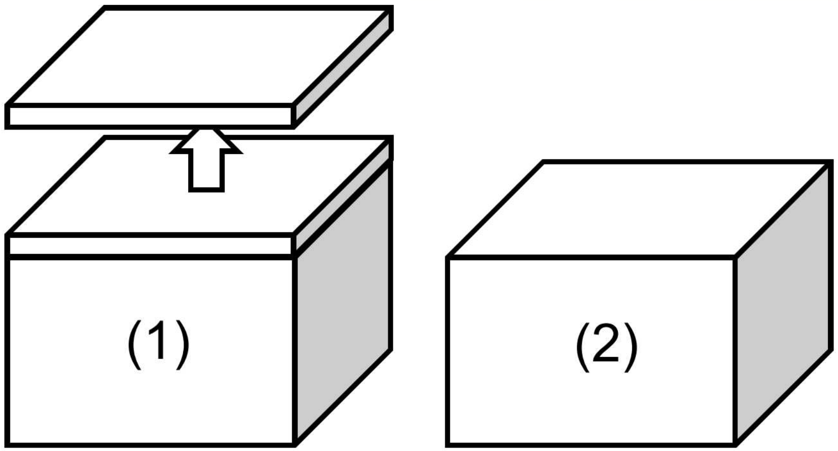

- Start with optically thick sample
- Removal of thin layer does not impact the reflectance of the sample
- Derive expression for Δreflectance → then set equal to 0

$$(\mu+\mu_0)R^m(\mu,\mu_0)=\frac{\varpi}{4}P^m(-\mu,\mu_0)+\frac{\varpi}{2}\mu_0\int_0^1 P^m(\mu,\mu')\,R^m(\mu',\mu_0)\,d\mu'$$
$$+\frac{\varpi}{2}\mu\int_0^1 R^m(\mu,\mu')\,P^m(\mu',\mu_0)\,d\mu'$$
$$+\varpi\mu\mu_0\int_0^1\int_0^1 R^m(\mu,\mu')\,P^m(-\mu',\mu'')\cdot R^m(\mu'',\mu_0)\,d\mu'\,d\mu''$$

μ: $|\cos(\theta_{\text{observation}})|$

μ_0: $|\cos(\theta_{\text{incident}})|$

E. G. Yanovitskij, *Light scattering in Inhomogeneous Atmospheres*, Trans. by S. Ginsheimer and O. Yanovitskij, Springer (1997).

Fourier coefficients of particle scattering function — **Single scattering albedo**

$P^m, \varpi \longrightarrow R^m$

Solution Provided by Michael Mishchenko (NASA GISS)

PERGAMON

Journal of Quantitative Spectroscopy & Radiative Transfer 63 (1999) 409–432

Journal of Quantitative Spectroscopy & Radiative Transfer

www.elsevier.com/locate/jqsrt

Bidirectional reflectance of flat, optically thick particulate layers: an efficient radiative transfer solution and applications to snow and soil surfaces

Michael I. Mishchenko[a,*], Janna M. Dlugach[b], Edgard G. Yanovitskij[b], Nadia T. Zakharova[c]

[a] *NASA Goddard Institute for Space Studies, 2880 Broadway, New York, NY 10025, USA*
[b] *Laboratory for Radiative Transfer Theory, The Main Astronomical Observatory, Ukrainian National Academy of Sciences, Golosiiv, 252650 Kyiv-22, Ukraine*
[c] *Science Systems and Applications, Incorporated, 2880 Broadway, New York, NY 10025, USA*

Abstract

We describe a simple and highly efficient and accurate radiative transfer technique for computing bidirectional reflectance of a macroscopically flat scattering layer composed of nonabsorbing or weakly absorbing, arbitrarily shaped, randomly oriented and randomly distributed particles. The layer is assumed to be homogeneous and optically semi-infinite, and the bidirectional reflection function (BRF) is found by a simple iterative solution of the Ambartsumian's nonlinear integral equation. As an exact solution of the radiative transfer equation, the reflection function thus obtained fully obeys the fundamental physical laws of energy conservation and reciprocity. Since this technique bypasses the computation of the internal radiation field, it is by far the fastest numerical approach available and can be used as an ideal input for Monte Carlo procedures calculating BRFs of scattering layers with macroscopically rough surfaces. Although the effects of packing density and coherent backscattering are currently neglected, they can also be incorporated. The FORTRAN implementation of the technique is available on the World Wide Web at http://www.giss.nasa.gov/ ~ crmim/brf.html and can be applied to a wide range of remote sensing, engineering, and biophysical problems. We also examine the potential effect of ice crystal shape on the bidirectional reflectance of flat snow surfaces and the applicability of the Henyey–Greenstein phase function and the δ-Eddington approximation in calculations for soil surfaces. © 1999 Elsevier Science Ltd. All rights reserved.

* Corresponding author. Tel.: + 212-678-5590; fax: + 212-678-6522
E-mail address: crmim@giss.nasa.gov (M.I. Mishchenko)

PII: S0022-4073(99)00028-X

National Aeronautics and Space Administration
Goddard Institute for Space Studies

Goddard Space Flight Center
Sciences and Exploration Directorate
Earth Sciences Division

- GISS Home
- News & Features
- Projects & Groups
- Datasets & Images
- Publications
- Software
- Education
- Events
- About GISS

Electromagnetic Scattering by Particles and Surfaces

FORTRAN Codes for the Computation of the Bidirectional Reflection Function for Flat Particulate Layers and Rough Surfaces

By Michael I. Mishchenko and Nadia T. Zakharova

This webpage provides access to two collections of FORTRAN codes.

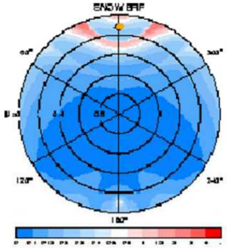

The first one can be used to compute the (scalar) bidirectional reflectance of a semi-infinite homogeneous slab composed of arbitrarily shaped, randomly oriented particles based on a rigorous numerical solution of the radiative transfer equation.

The second one can be used to compute the Stokes reflection matrix of a rough interface separating two homogeneous half-spaces with different refractive indices (e.g., a rough ocean surface).

Particulate Semi-Infinite Layers
The code brf.f solves the Ambartsumian's nonlinear integral equation for the reflection function using a simple iterative method. Since this technique bypasses the computation of the internal field, it is by far the fastest and most accurate numerical approach available.

The codes are ideally suitable to computing the BRF for flat snow, soil, and powder surfaces and optically thick clouds and may find applications in geophysics, physics, biophysics, and industrial research.

A detailed user manual to the codes has been published: M. I. Mishchenko, J. M. Dlugach, E. G. Yanovitskij, and N. T. Zakharova, Bidirectional reflectance of flat, optically thick particulate layers: An efficient radiative transfer solution and applications to snow and soil surfaces, *J. Quant. Spectrosc. Radiat. Transfer*, **63**, 409-432 (1999). A hardcopy reprint of this paper is available from Michael Mishchenko upon request. Please leave a message at mmishchenko@giss.nasa.gov indicating your name and mailing address.

The users of the codes are encouraged to visit this page on a regular basis for information on latests developments, warnings, and/or errors found. We would highly appreciate informing us of any problems and errors encountered with these codes. Please e-mail your questions and comments to mmishchenko@giss.nasa.gov.

FORTRAN codes
To retrieve a code, click on the code name and use the "Save As..." option from the "File" menu.

- refl.f - This code computes Fourier components of the reflection function
- interp.f - This code computes the bidirectional reflection function for a given set of scattering geometries
- spher.f - This code computes the Legendre expansion coefficients for polydisperse spherical particles using the standard Lorenz-Mie theory

The codes must be run in the following sequence: spher.f -> refl.f -> interp.f.

Note that the Legendre expansion coefficients for polydisperse, randomly oriented nonspherical particles and sphere aggregates can be computed using O T-matrix codes also available on this website. The expansion coefficients for the standard and double-peaked Henyey-Greenstein phase functions are computed using Eqs. (15) and (19) of the manual. Below we also provide the Legendre expansion coefficients for two nonspherical ice particle models described in the manual.

Benchmark results
The following output files were computed by the codes in their current settings and may provide a useful test of the performance of the codes on different computers:

- spher.print
- spher.write
- refl.print
- interp.write

The file refl.write is not given here because of its large size.

Solution Provided by Michael Mishchenko (NASA GISS)

Step #1: n, k + 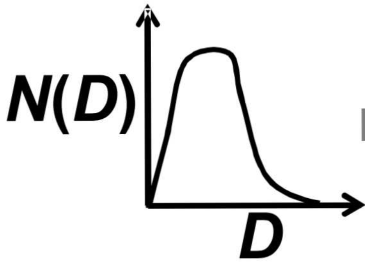

$\rightarrow$ $P^m, \tilde{\omega}$

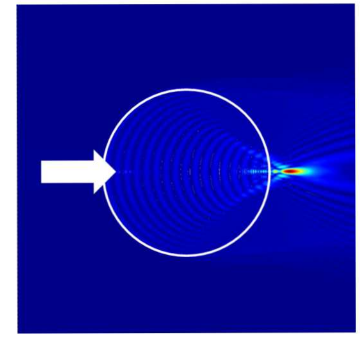

Step #2: $P^m, \tilde{\omega} \rightarrow R^m$

$$\begin{aligned}(\mu+\mu_0)R^m(\mu,\mu_0) &= \frac{\varpi}{4}P^m(-\mu,\mu_0)+\frac{\varpi}{2}\mu_0\int_0^1 P^m(\mu,\mu')\,R^m(\mu',\mu_0)\,d\mu' \\ &+\frac{\varpi}{2}\mu\int_0^1 R^m(\mu,\mu')\,P^m(\mu',\mu_0)\,d\mu' \\ &+\varpi\mu\mu_0\int_0^1\int_0^1 R^m(\mu,\mu')\,P^m(-\mu',\mu'')\cdot R^m(\mu'',\mu_0)\,d\mu'\,d\mu''\end{aligned}$$

Step #3:

$$\begin{cases} R(\mu,\mu_0,\varphi) = R^0(\mu,\mu_0) + 2\sum_{m=1}^{m_{\max}} R^m(\mu,\mu_0)\cos(m\varphi) \\ \text{Plane albedo}(\mu_0) = 2\int_0^1 R^0(\mu,\mu_0)\,\mu\,d\mu \end{cases}$$

Our Canonical Geometry: Spheroids

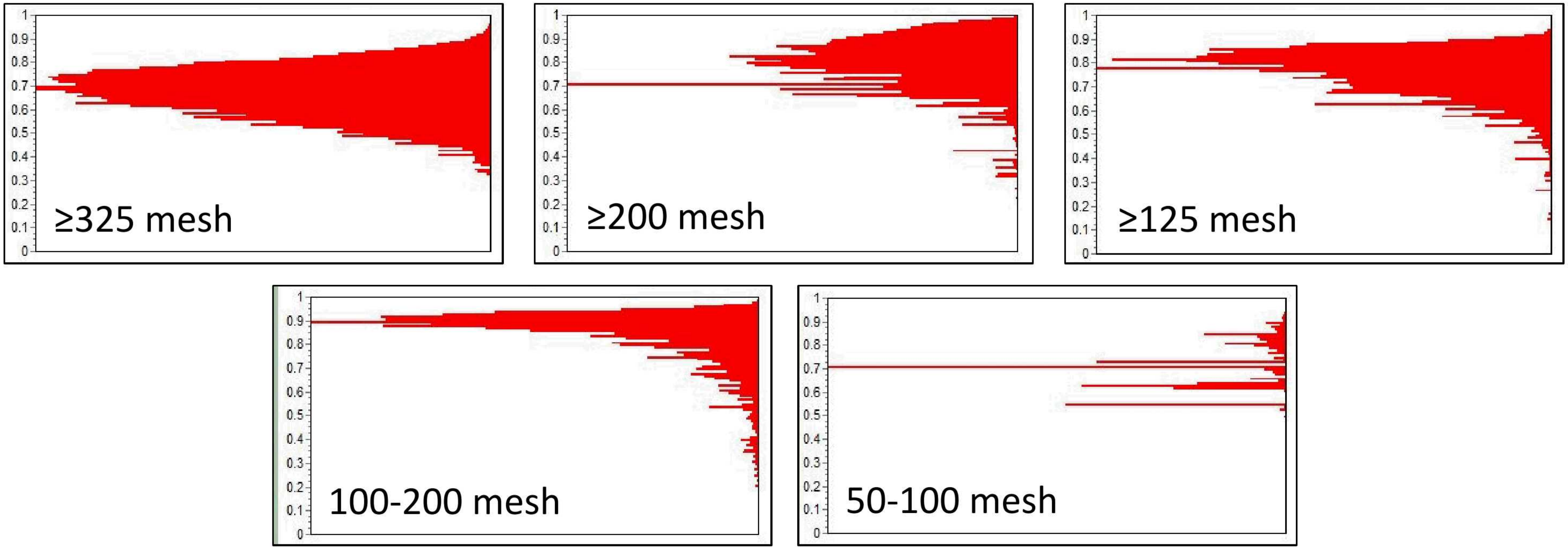

- This range of shapes and aspect ratios (ARs) is greatly simplified
- Shape = spheroid, AR = one characteristic value
- 2 shape bins: one bin each per prolate, oblate

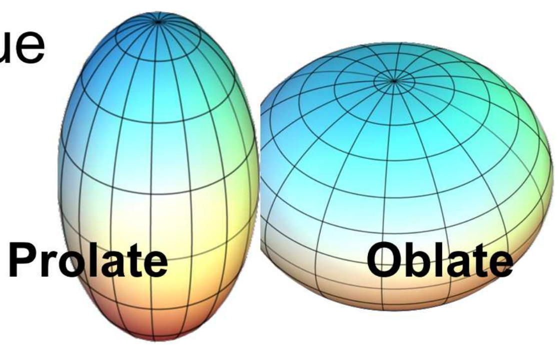

Calculating P^m, $\tilde{\omega}$

Pergamon

PII: S0022-4073(98)00008-9

J. Quant. Spectrosc. Radiat. Transfer Vol. 60, No. 3, pp. 309–324, 1998
Published by Elsevier Science Ltd
Printed in Great Britain
0022-4073/98 $19.00 + 0.00

CAPITABILITIES AND LIMITATIONS OF A CURRENT FORTRAN IMPLEMENTATION OF THE *T*-MATRIX METHOD FOR RANDOMLY ORIENTED, ROTATIONALLY SYMMETRIC SCATTERERS

MICHAEL I. MISHCHENKO† and LARRY D. TRAVIS
NASA Goddard Institute for Space Studies, 2880 Broadway, New York, New York 10025, U.S.A.

Abstract—We describe in detail a software implementation of a current version of the *T*-matrix method for computing light scattering by polydisperse, randomly oriented, rotationally symmetric particles. The FORTRAN *T*-matrix codes are publicly available on the World Wide

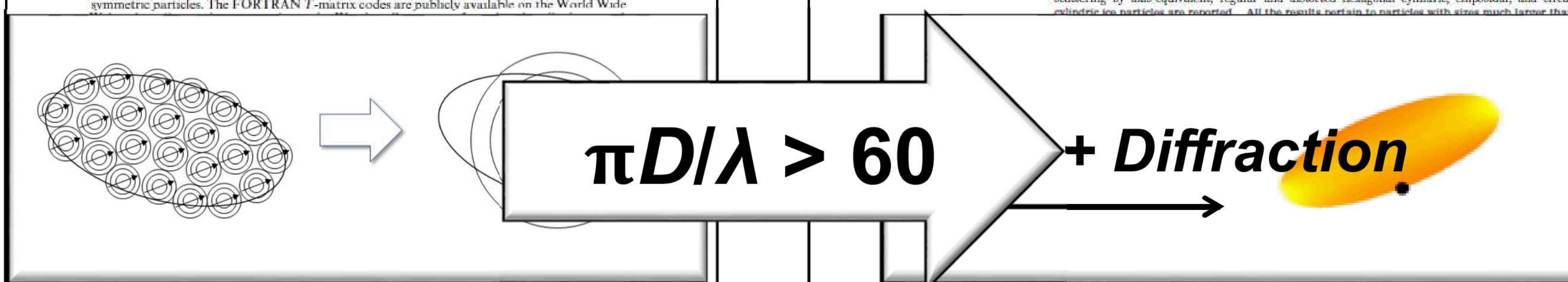

procedure convenient in massive computer calculations for particle polydispersions, and Ref. 5 presents benchmark *T*-matrix computations for particles with non-smooth surfaces (finite circular cylinders). A general review of the *T*-matrix method can be found in Ref. 7.

In this paper we provide a detailed description of modern *T*-matrix FORTRAN codes which incorporate all recent developments, are publicly available on the World Wide Web, and are, apparently, the most efficient and powerful tool for accurately computing light scattering by randomly oriented rotationally symmetric particles. For the first time, we collect in one place all necessary formulas, discuss numerical aspects for *T*-matrix computations, describe the input and output parameters, and demonstrate the capabilities and limitations of the codes. The paper is intended to serve as a detailed user guide to a versatile tool suitable for a wide range of practical applications. We specifically target the users who are interested in practical applications of the *T*-matrix method rather than in details of its mathematical formulation.

2. BASIC DEFINITIONS

The single scattering of light by a small-volume element dv consisting of randomly oriented, rotationally symmetric, independently scattering particles is completely described by the ensemble-averaged extinction, C_{ext}, and scattering, C_{sca}, cross sections per particle and the dimensionless

† Author to whom correspondence should be addressed.

Applicability of regular particle shapes in light scattering calculations for atmospheric ice particles

Andreas Macke and Michael I. Mishchenko

We ascertain the usefulness of simple ice particle geometries for modeling the intensity distribution of light scattering by atmospheric ice particles. To this end, similarities and differences in light scattering by axis-equivalent, regular and distorted hexagonal cylindric, ellipsoidal, and circular cylindric ice particles are reported. All the results pertain to particles with sizes much larger than a

erably larger than the wavelengths of the incoming solar radiation, especially in the visible spectral region. Therefore, the geometrical optics approximation offers a conceptually simple although time-consuming way to simulate single scattering by almost arbitrarily shaped scatterers.[1–5] Whereas these papers take more and more complex particle geometries such as bullet rosettes, dendrites, or polycrystals into account, in this paper we examine the possibility of representing the scattering proper-

The authors are with the NASA Goddard Institute for Space Studies, 2880 Broadway, New York, New York 10025. A. Macke is also with the Department of Applied Physics, Columbia University, 2880 Broadway, New York, New York 10025. M. I. Mishchenko is also with the Institute of Terrestrial and Planetary Atmospheres, State University of New York at Stony Brook, Stony Brook, New York 11794.

Received 28 August 1995; revised manuscript received 29 January 1996.
0003-6935/96/214291-06$10.00/0

On the other hand, the three (two) semiaxes of an ellipsoid (circular cylinder) allow for a variability of particle shapes that may cover to some extent the natural variability of atmospheric ice crystal habits.

Another motivation arises from uncertainties in our knowledge of real ice particle shapes. The study of observationally derived two-dimensional ice crystal shadow images[6] or replicas[7,8] clearly demonstrates that solid hexagonal columns or plates are a strong idealization of atmospheric ice crystals. However, statistically reliable shape information is difficult to extract from these data, partly because of the strong natural variability. Therefore it appears reasonable to ascertain the use of nonhexagonal but still simple geometries as substitutes for a polydisperse sion of complicated ice particle shapes.

Because of the lack of sharp edges, ellipsoids do not provide strong halos that are characteristic of regular hexagonal particles. However, the absence of these features, as reported in a number of radiance measurements in or above cirrus clouds,[9,10] emphasizes the potential use of nonhexagonal par-

1^{st}-Surface Reflectance and Surface Roughness

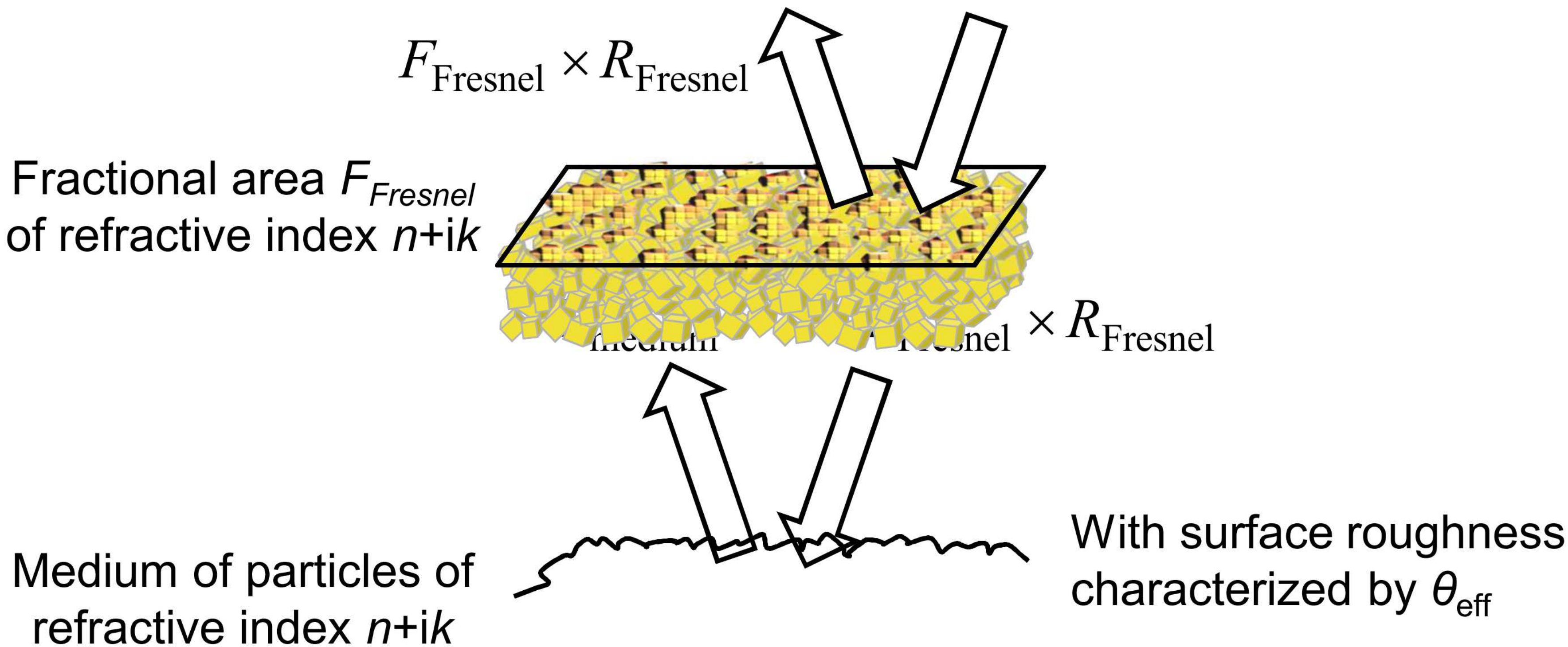

$$R = F_{\text{Fresnel}} \times R_{\text{Fresnel}} + \left(1 - F_{\text{Fresnel}} \times R_{\text{Fresnel}}\right) \times R_{\text{medium}}$$

Full Characterization of Material Systems

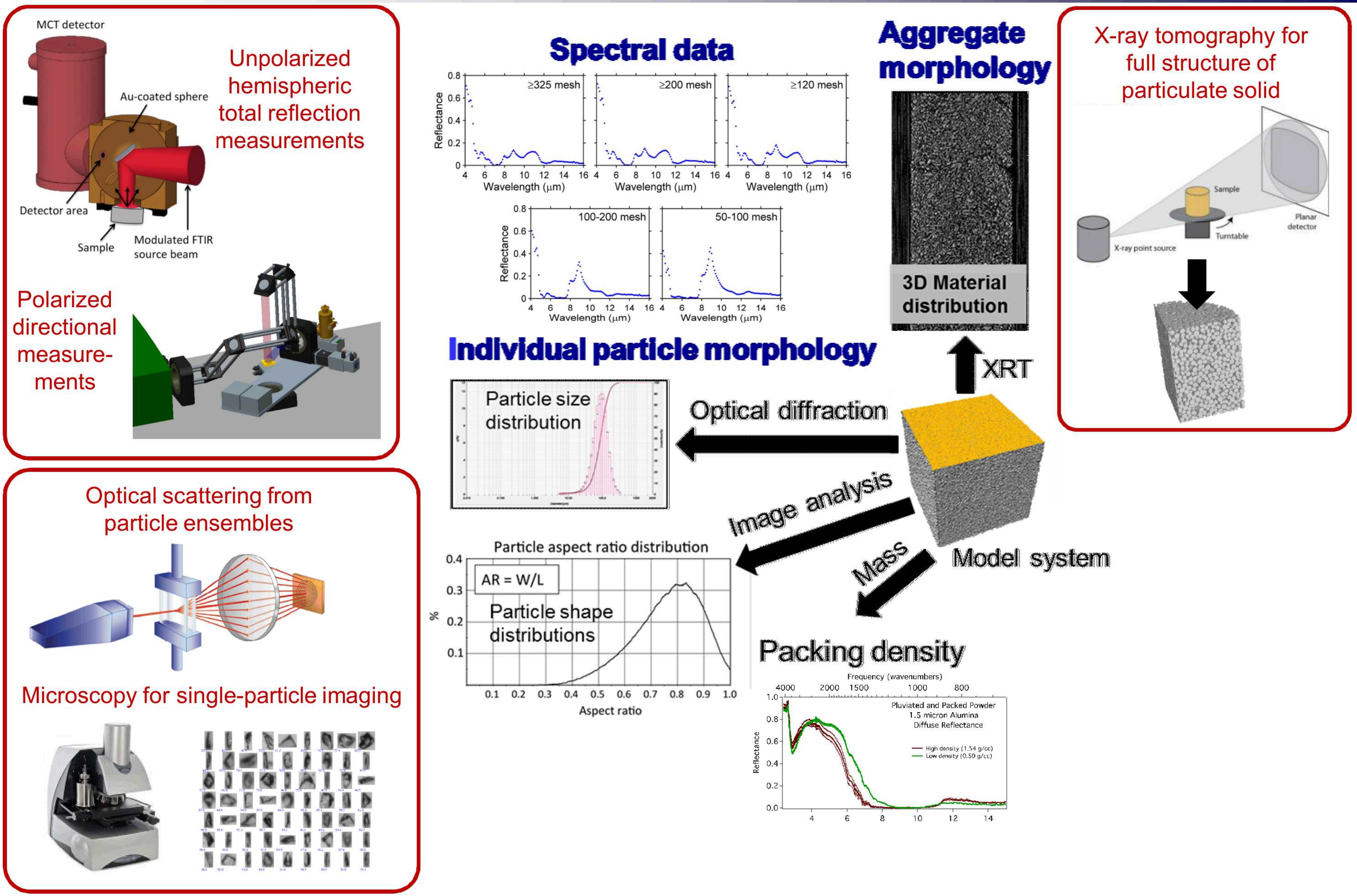

Model Assessment

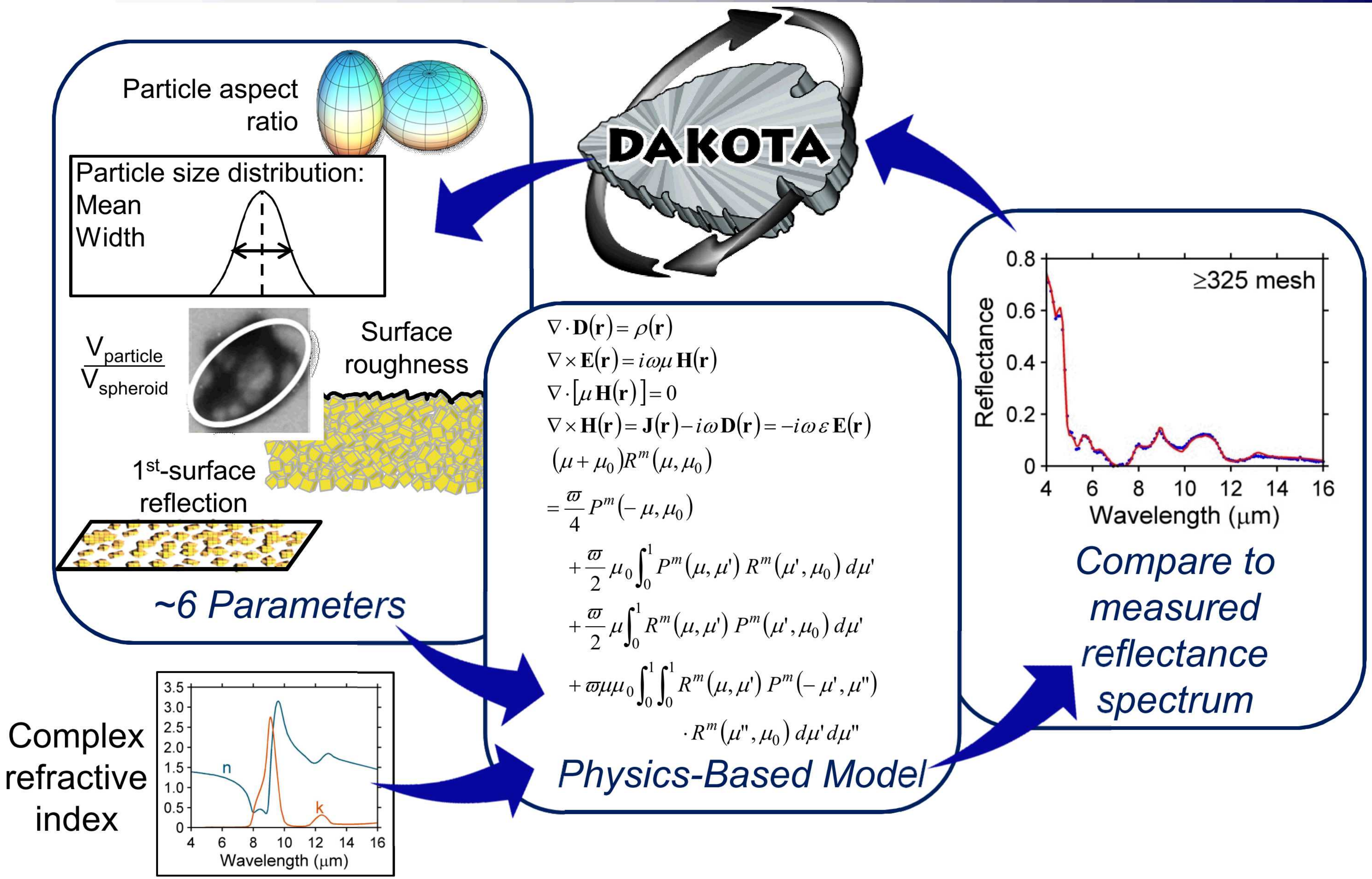

Measured and Modeled Reflectance Spectra of Silica Powders

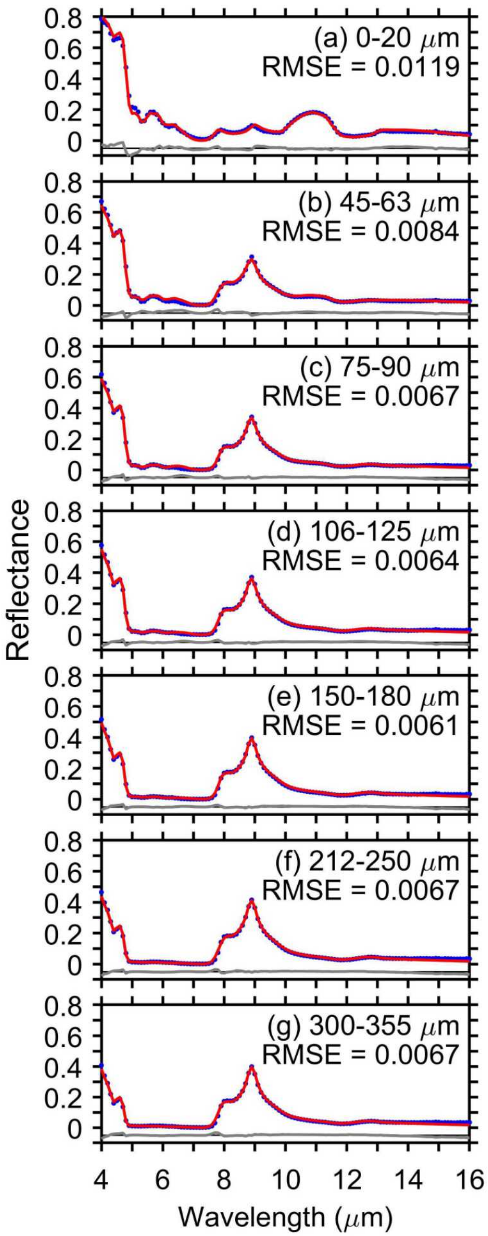

Nice agreement, but…

"Give me seven free parameters and I can fit an elephant"

– K. Lumme and A. Penttilä, JQSRT **112**, 1658-1670 (2011).

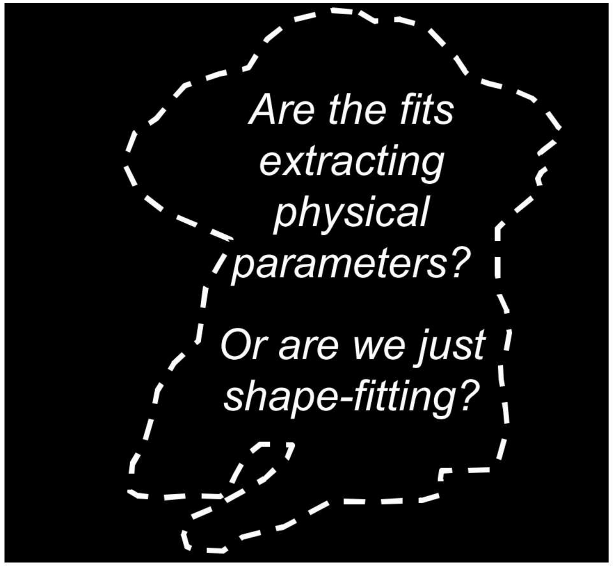

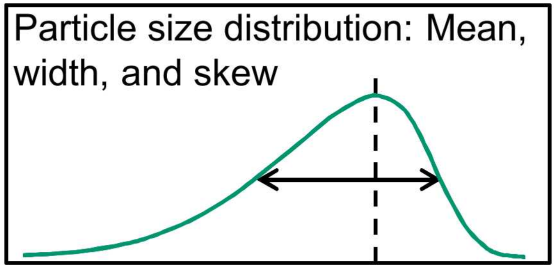

VS

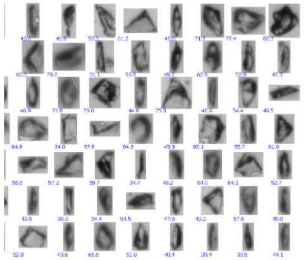

Measured and Modeled Reflectance Spectra and PSDs of Silica Powders

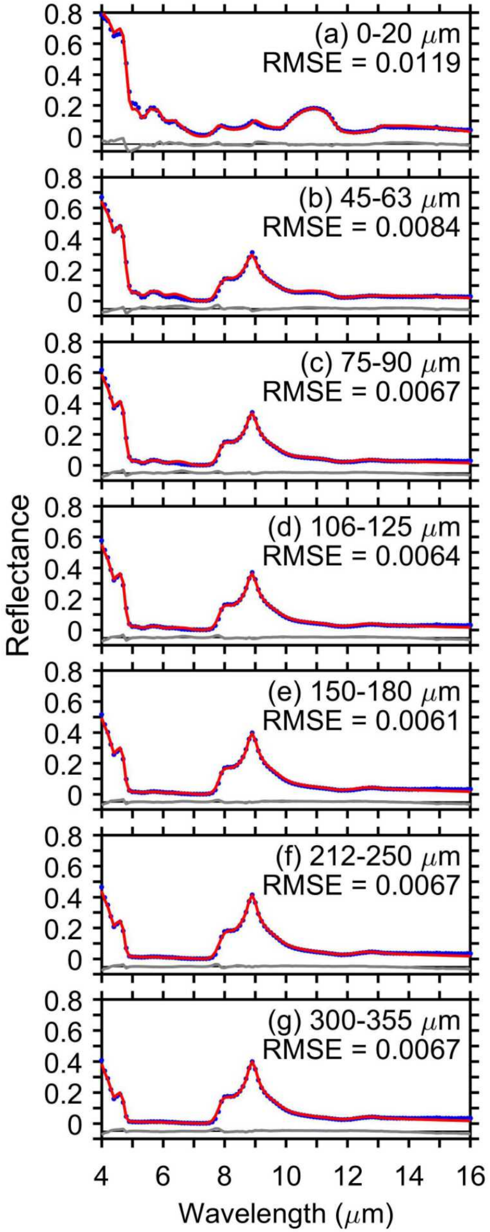

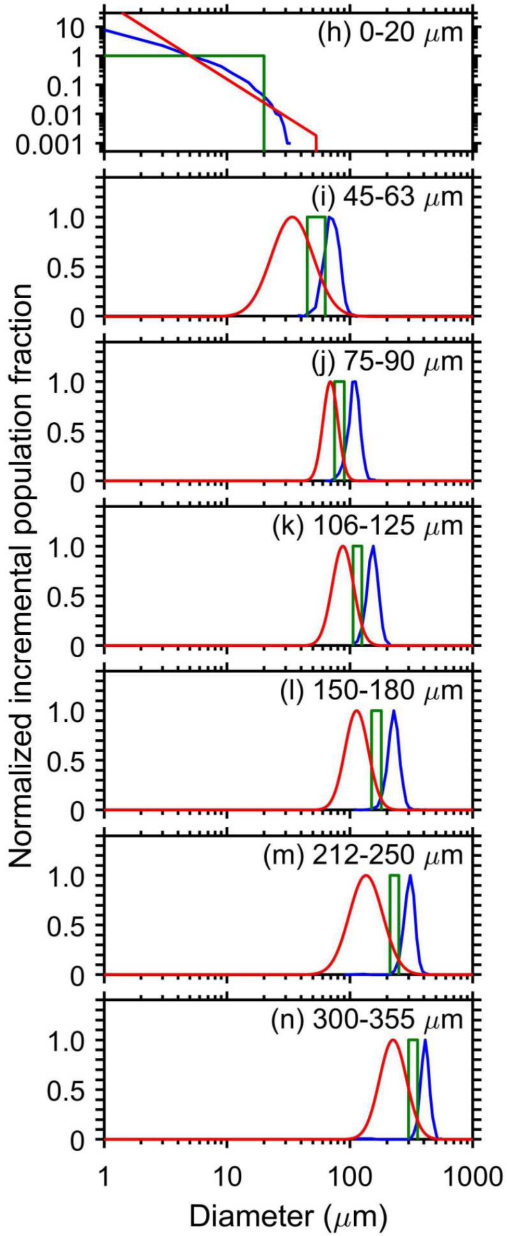

- Departure from measured PSDs is evident
  - Model-derived PSDs are skewed to smaller particle sizes
- Potential cause: The reflectance of larger particles is spectrally similar to the R_{Fresnel} of the bulk material
  - Optimization is likely attributing reflectance contribution of larger particles to 1st-surface reflectance term

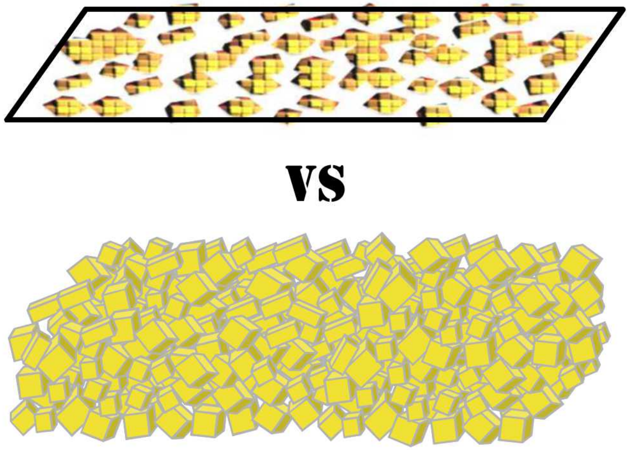

Recall phenomenological "surface scattering" vs. "volume scattering"

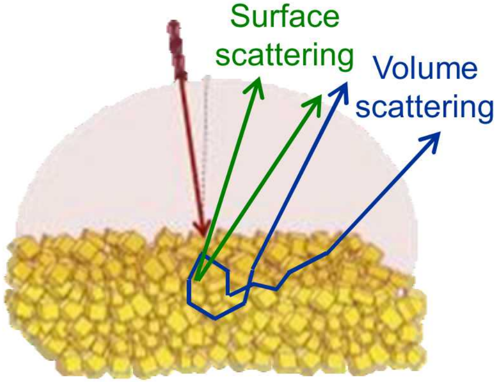

Surface scattering from particles: High k

Volume scattering from particles: Low k

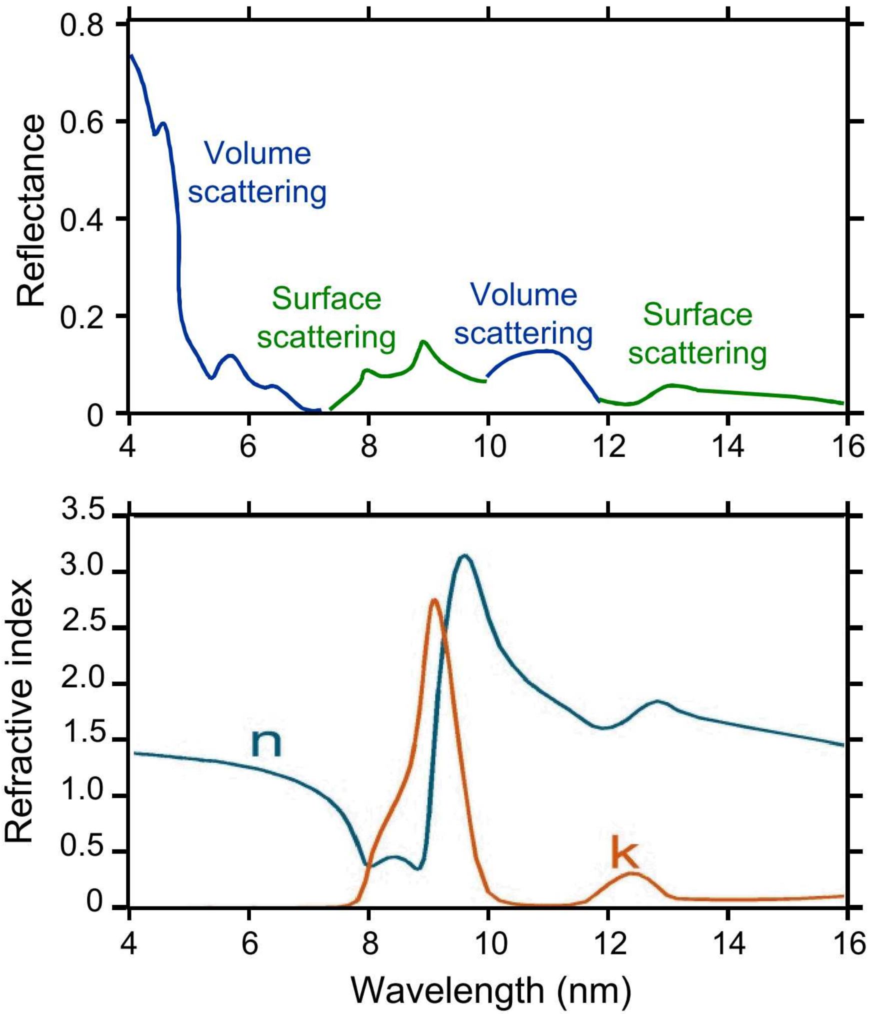

Now consider *optically thin* (vs. optically thick) deposits

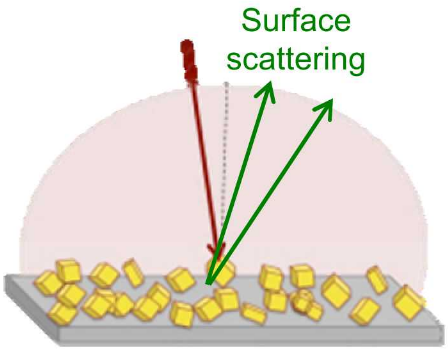

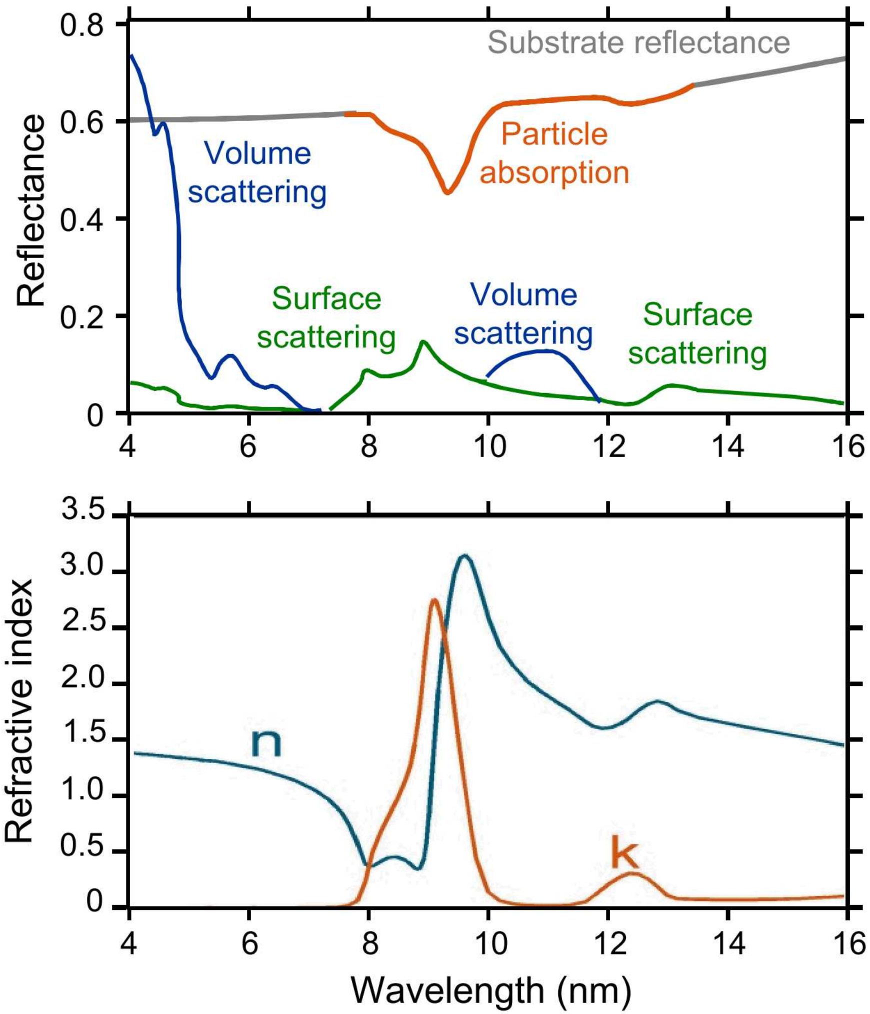

Surface scattering from particles: High k

Volume scattering from particles: Low k

1) *Volume*-scattering features will effectively disappear.
2) *Surface* scattering remains, but (for small particles) the substrate will be its primary source.
3) For small particles, the spectrum will appear similar to the substrate reflectance, but attenuated by particle absorption (defined by *k*).

Computational Approach: The Adding-Doubling Method

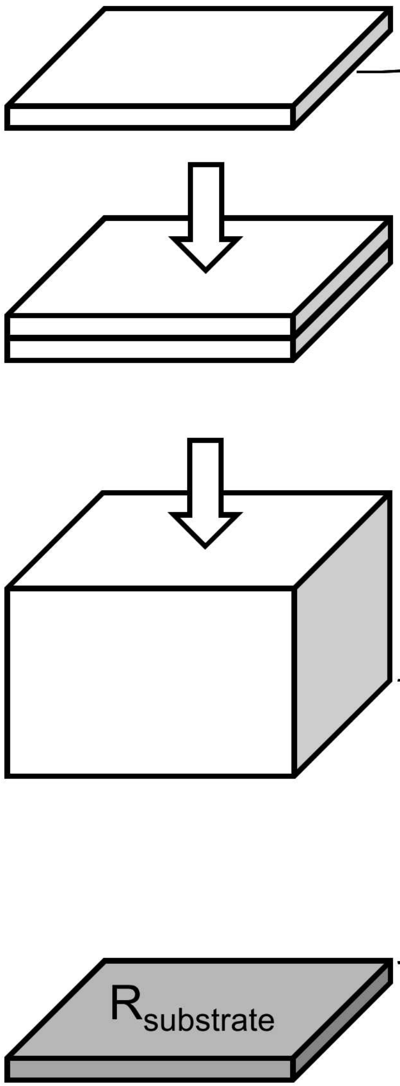

$$P^m(\mu,\mu_0),\varpi \Rightarrow R^m(\tau;\mu,\mu_0),\ T^m(\tau;\mu,\mu_0)$$

Coefficients of scattering function	Single scattering albedo	Reflection function	Transmission function

optical thickness 2τ $\Rightarrow R^m(2\tau;\mu,\mu_0),\ T^m(2\tau;\mu,\mu_0)$

$$R^m(2\tau;\mu,\mu_0)=R^m(\tau;\mu,\mu_0)+\exp(-\tau/\mu)\,U(\mu,\mu_0)+2\int_0^1 T^m(\tau;\mu,\mu')\,U(\mu',\mu_0)\,\mu'\,d\mu'$$

$$T^m(2\tau;\mu,\mu_0)=\exp(-\tau/\mu)D(\mu,\mu_0)+T^m(\tau;\mu,\mu_0)\exp(-\tau/\mu)+2\int_0^1 T^m(\tau;\mu,\mu')\,D(\mu',\mu_0)\,\mu'\,d\mu'$$

$$Q_1(\mu,\mu_0)=2\int_0^1 R^m(\tau;\mu,\mu')\,R^m(\tau;\mu',\mu_0)\,\mu'\,d\mu';\ Q_n(\mu,\mu_0)=2\int_0^1 Q_1(\mu,\mu')\,Q_{n-1}(\mu',\mu_0)\,\mu'\,d\mu'\quad(n\ge 2)$$

$$S(\mu,\mu_0)=\sum_{n=1}^{\infty}Q_n(\mu,\mu_0);\ D(\mu,\mu_0)=T^m(\tau;\mu,\mu_0)+S(\mu,\mu_0)\exp(-\tau/\mu_0)+2\int_0^1 S(\mu,\mu')T^m(\tau;\mu',\mu_0)\,\mu'\,d\mu'$$

$$U(\mu,\mu_0)=R^m(\tau;\mu,\mu_0)\exp(-\tau/\mu_0)+2\int_0^1 R^m(\tau;\mu,\mu')D(\mu',\mu_0)\,\mu'\,d\mu'$$

$$R_S^0(\Delta\tau;\mu,\mu_0)=R^0(\Delta\tau;\mu,\mu_0)+\frac{R_{\text{substrate}}}{1-R_{\text{substrate}}A_{\text{layer}}}\,t_a(\mu)\,t_a(\mu_0)$$

$$A_{\text{layer}}=4\int_0^1\int_0^1 R^0(\Delta\tau;\mu,\mu_0)\,\mu\,\mu_0\,d\mu\,d\mu_0;\ t_a(\mu)=\exp(-\Delta\tau/\mu)+2\int_0^1 T^0(\Delta\tau;\mu,\mu')\,\mu'\,d\mu'$$

Initial Analysis of Optically Thin Deposits

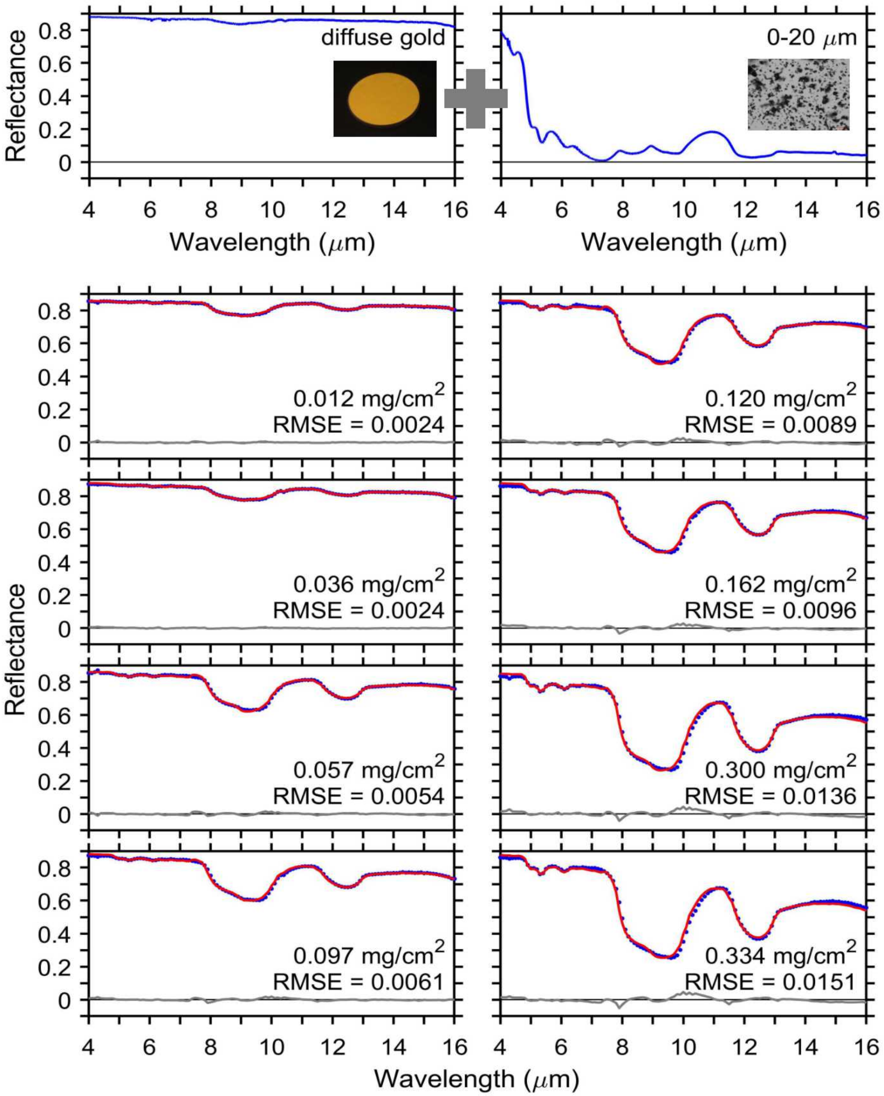

- Acquired measurements of size-selected fused silica powders deposited on two different substrates at multiple mass loadings (mg/cm^2)
  - Diffuse gold → High albedo, spectrally flat (representative of metallic surfaces)
  - Polycarbonate → Low albedo, spectrally featured (representative of plastic surfaces)
- Numerically inverted model effectively captures the spectral features of these optically thin deposits
- Model effectively extracts mg/cm^2 of the deposits as well.

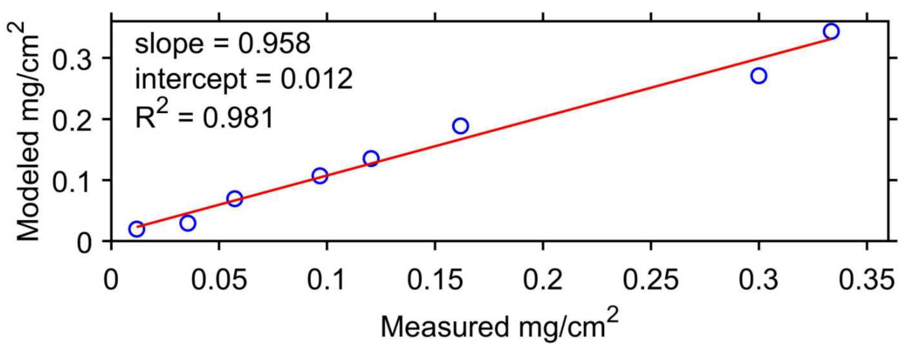

Q: What is the related impact on *Bio*(Nuclear Working Group)?
A: LWIR sensing of vegetation

- RT approaches are already integrated into various community models
  - PROSPECT (Jacquemond and Baret, Rem. Sens. Environ. **34**, 75-91, 1990)
  - LIBERTY: Leaf Incorporating Biochemistry Exhibiting Reflectance and Transmittance Yields (Dawson et al., Rem. Sens. Environ. **65**, 50-60, 1998)
  - DLM: Dorsiventral Leaf radiative transfer Model (Stuckens et al., Rem. Sens. Environ., **113**, 2560-2573, 2009)
  - SCOPE: Soil Canopy Observation, Photochemistry and Energy fluxes (van der Tol et al., Biogeosceinces **6**, 3109-3129 (2009).
  - FluorMODleaf (Pedros et al., Rem. Sens. Environ. **114**, 155-167, 2010)
  - DART: Discrete Anisotropic Radiative Transfer (Gastellu-Etchegorry et al., InTech 2012)
  - COSINE: ClOse-range Spectral ImagiNg of lEaves (Jay et al., Rem. Sens. Environ. **177**, 220-236, 2016)
  - Fluspect-B (Vilfan et al., Rem. Sens. Environ. **186**, 596-615, 2016)
  - FluorWPS (Zhao et al., Rem. Sens. Environ. **187**, 385-399, 2016)
- LWIR data are now being exploited to identify/characterize vegetation
  - "…where spectral features seem to be mainly associated with the biochemical composition of the leaf surface" (Gerber et al., Rem. Sens. Environ. **115**, 404-414, 2011).
- Therefore need robust signature models applicable to the LWIR
  - Extension to LWIR will increase important of capturing morphological impact

Q: What is the related impact on *Bio*(Nuclear Working Group)?
A: LWIR sensing of biological soil crusts

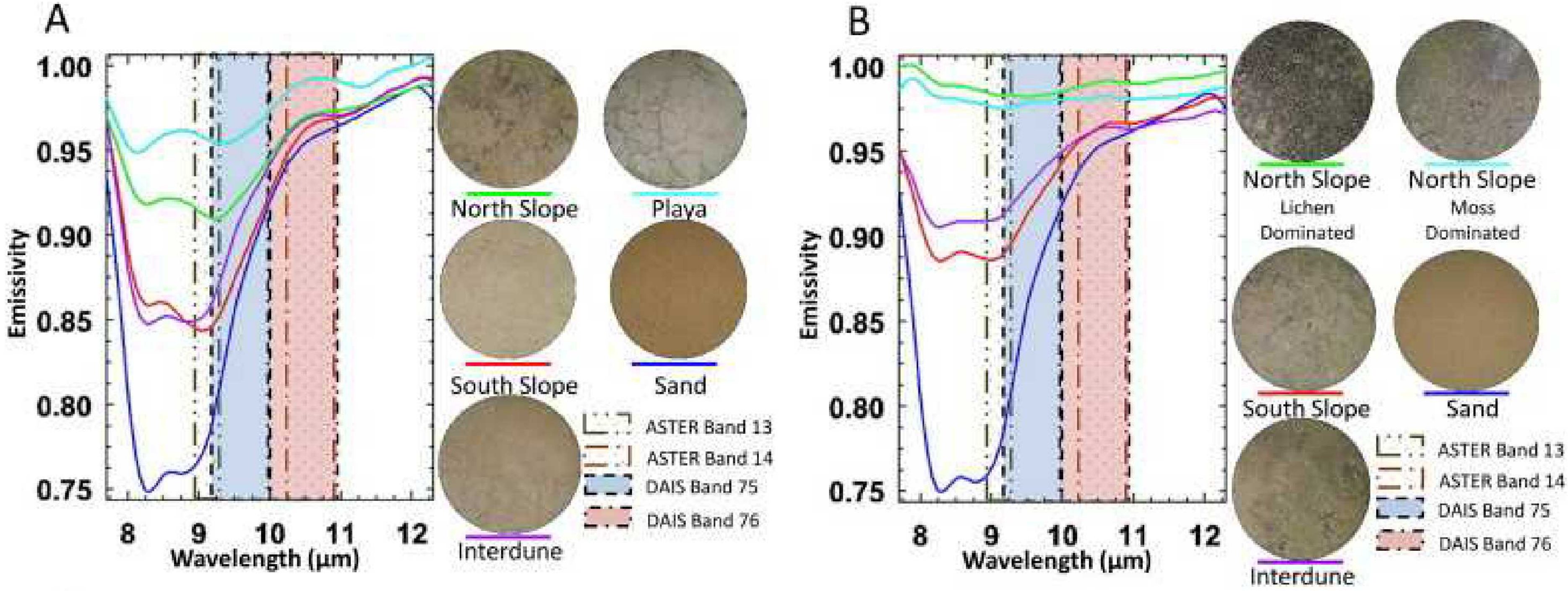

O. Rozenstein and A. Karnieli, "Identification and characterization of Biological Soil Crusts in a sand dune desert environment across Israel-Egypt border using LWIR emittance spectroscopy," J. Arid Environ. **112**, 75-86, 2015.

Summary and Takeaways

- Material reflectance signatures are dependent upon morphology
- This morphological dependence can be captured via modeling
- Potential of applying such models to biological systems largely unexplored

Acknowledgments

- Work funded under the HARD Solids Venture by the DOE Office of Defense Nuclear Nonproliferation R&D (DNN R&D)
- Michael Mishchenko (NASA GISS) – Modeling advice and assistance
- Patty Hough (Sandia National Laboratories, CA) – Model inversion via Dakota, parallel computing

Thanks! Questions?

Extra Viewgraphs

Optimization via "nl2sol" in DAKOTA

- 121 λs: 4-16 μm @ 0.1 μm resolution
- The 121 λ-dependent calculations are divided among 64 processors (4 nodes, 16 cores/node)
- ~10 min/spectrum, 100+ such calculations required for convergence

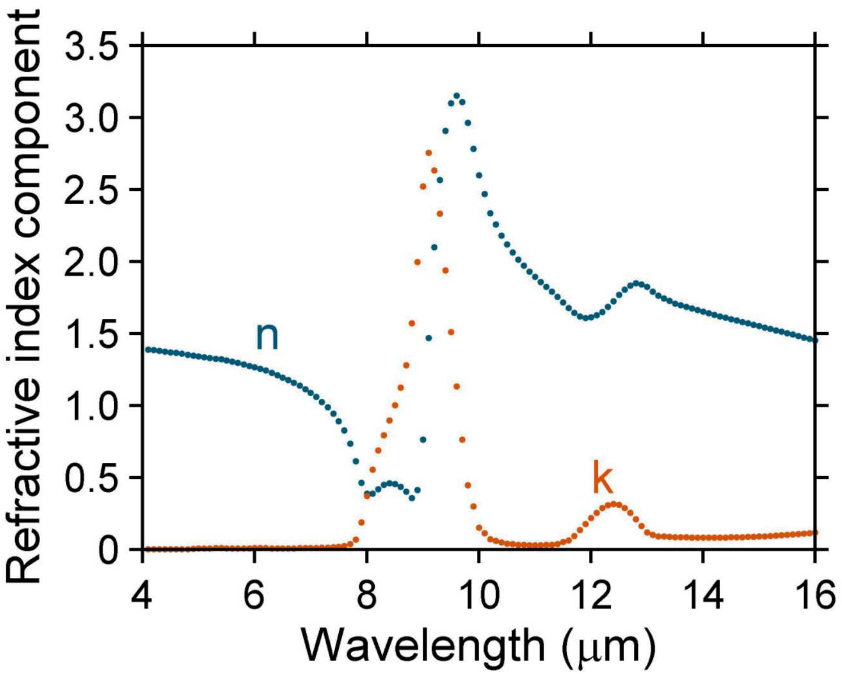

- The Jacobian (matrix of 1st-order partial derivatives) is numerically determined through forward difference calculations
- The Hessian (matrix of 2nd-order partial derivatives) is numerically approximated from special properties of the sum-of-squares

T-matrix vs. Ray tracing

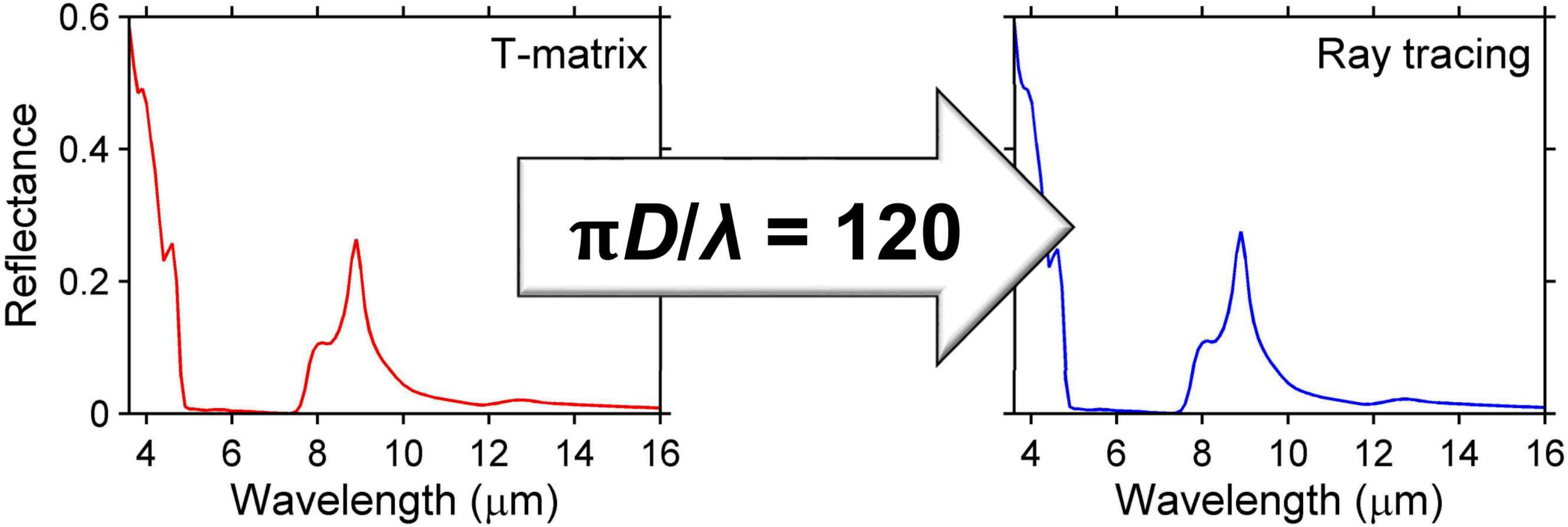

T-matrix vs. Ray tracing

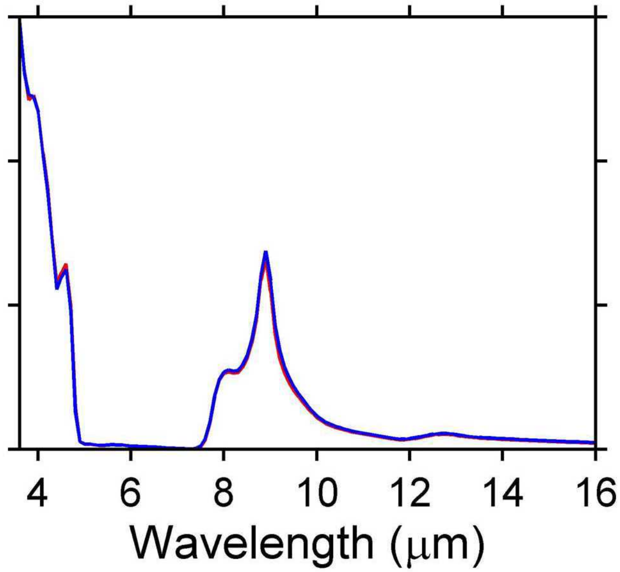

Similar Approximations Made by Others

- J. L. Bandfield, P. O. Hayne, J.-P. Williams, B. T. Greenhagen, and D. A. Paige, “Lunar surface roughness derived from LRO Diviner Radiometer observations,” Icarus **248**, 357-372 (2015).
- P. Helfenstein and M. K. Shepard, “Submillimeter-scale topography of the lunar regolith,” Icarus **141**, 107-131 (1999).
- M. K. Shepard, R. A. Brackett, and R. E. Arvidson, “Self-affine (fractal) topography: Surface parameterization and radar scattering,” J. Geophys. Res. **100**, 11709-11718 (1995).
- B. Hapke, “Bidirectional reflectance spectroscopy. 3. Correction for Macroscopic Roughness,” Icarus **59**, 41-59 (1984).

But is this approximation sufficient?